Creep Rupture of a Metal-ceramic Particulate Composite

T. -J. CHUANG, D. F. CARROLL and S. M. WIEDERHORN

Ceramics Division, National Institute of Standards and Technology, Gaithersburg, MD 20899, USA

ABSTRACT

The creep rupture behavior of a ceramic particulate composite system was studied under tensile and flexural loading. The rupture process commences from the heterogeneous formation of cavities at particle interfaces in the tensile stress field. As deformation proceeds, a critical strain is reached whereupon cavity coalescence takes place forming large microcracks. Ultimately, rupture occurs when one of these microcracks reaches a critical length and the remaining ligament cannot sustain the applied load. On the assumption that microcracks grow to a critical size through the coalescence of cavities, a new rupture criterion is proposed based upon a critical strain concept of failure. Using this criterion for fracture, together with a detailed creep mechanics analysis, theoretical predictions are made of lifetime under both bending and simple tension. Creep and creep rupture data for a grade of siliconized silicon carbide tested at 1300°C are collected and compared with the proposed theory. Reasonable agreement between theory and experiment were obtained in both modes of loading.

KEYWORDS

Creep rupture; lifetime prediction; bending rupture; tensile rupture; rupture criterion; damage-enhanced creep; asymmetric creep; ceramic composite.

INTRODUCTION

For load-carrying applications at elevated temperatures such as advanced heat engines and heat exchangers, high technology ceramics and composites have shown potential as next generation materials to compete with the conventional superalloys now in service. Ceramic particulate composites belong to this class of high performance structural ceramics. An example of this type of composite is siliconized silicon carbide (KX01)[1] -- a

[1]SOHIO Corp., Cleveland, OH. This brand name is supplied for identification only and does not imply endorsement by NIST.

two-phase composite fabricated by the infiltration of silicon metal into a porous silicon carbide preform. As a result of this processing technique, a composite is formed, consisting of ~33 vol % silicon metal embedded with 3-5 μm SiC particulates. A fully dense, relatively homogeneous microstructure is achieved, with high strength, toughness and creep resistance. Despite these promising features, confidence in the mechanical performance and final acceptance of this material must await the establishment of its long term reliability.

The purpose of this paper is to present theoretical and experimental work on the creep and rupture of siliconized silicon carbide subjected to simple tension, compression and bending. The creep response of this material to uniaxial loading will be discussed first. It is shown that the material obeys an asymmetric creep law distinct from the usual constitutive laws observed in metals or alloys[1-4]. A discussion is then presented of the physical processes that lead to rupture, from which a new failure criterion is proposed. Based on this criterion for rupture, a closed form expression for the rupture time, similar to the Monkman-Grant equation, is derived for tensile loading. In bending, however, the complexity of the stress state necessitates the use of a numerical approach to compute the total time to rupture as a function of applied bending moment. Experimental measurements of creep and rupture under both simple tension and flexural loading conditions were used to verify the theoretical predictions of lifetime. Reasonable agreement was obtained between theory and experiment.

ASYMMETRIC CREEP

To understand rupture behavior, the creep constitutive laws in various stress states must be experimentally determined, as the response of a material to creep exerts a great influence on the rupture behavior. In this regard, an experimental program was conducted in which uniaxial tensile tests and compressive creep tests were conducted. Detailed descriptions of the experimental procedures for creep testing are given in ref. [3]; the resulting data are quoted here.

Figures 1 and 2 show typical creep and creep rate data respectively for tensile and compressive loading. Two major features may be noted; a substantial asymmetry is observed between tension and compression tests of identical load (figure 2), in sharp contrast to conventional metal or alloy systems where the responses are comparable except the sign[1]; The roles played by primary and tertiary stages are minor in contrast to that observed in metals. Most of the specimens creep life is spent in the steady state creep regime (figure 1).

This behavior allows one to write the following approximate relation between final rupture strain, ϵ_f, steady state creep rate $\dot{\epsilon}_s$, and total time to rupture, t_f

$$\epsilon_f \approx \dot{\epsilon}_s \, t_f \ . \qquad (1)$$

The fact that the secondary creep dominates the creep process also means that $\dot{\epsilon}_s$ is the crucial parameter to characterize the creep behavior for long-term engineering applications.

The logarithm of $\dot{\epsilon}_s$ of the KX01 is plotted as the logarithm of the applied stress in figure 2. As can be seen, the creep curves for tension and compression are similar in appearance, but are displaced along the stress

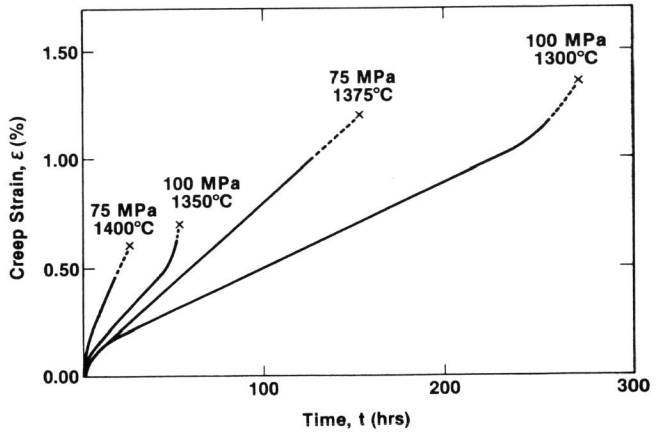

Figure 1. Uniaxial creep curves for KX01 at various thermal and mechanical loadings showing reducing steady-state creep rates with increasing rupture strains.

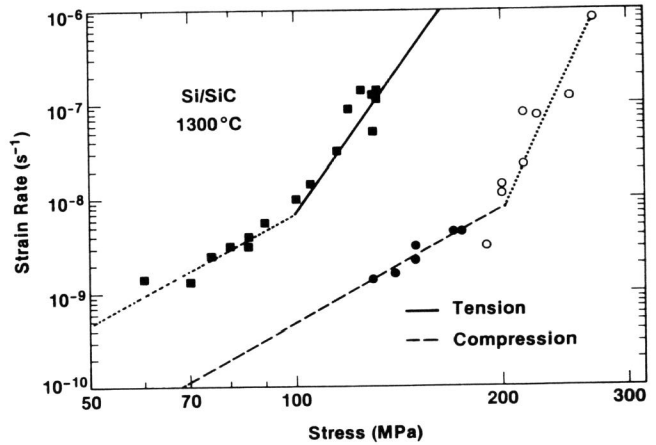

Figure 2. Creep rate versus stress relationship of KX01 indicating asymmetric creep between tension and compression. Dashed lines with a slope of 4 are due to dislocational creep; whereas solid line with a slope of 10 is due to cavitational damage[3-4].

axis; the stress required for a given strain rate is greater in compression than in tension. Both curves are bimodal, having stress exponents of approximately 4 at low strain rates and approximately 10 at high strain rates. For simple tension, the following equations describe the creep rate:

$$\text{for} \quad \sigma_a > \sigma_o \qquad \dot{\epsilon}_s = \dot{\epsilon}_o \, (\sigma_a/\sigma_o)^N \tag{2a}$$

$$\text{for} \quad \sigma_a < \sigma_o \qquad \dot{\epsilon}_s = \dot{\epsilon}_o \, (\sigma_a/\sigma_o)^n \tag{2b}$$

where σ_a is the applied stress; σ_o is threshold stress above which damage accumulation in the form of cavities occurs, $\dot{\epsilon}_o$ is the creep rate at $\sigma = \sigma_o$; N is the stress exponent in the regime of cavitation whereas, n is the stress exponent in the regime where no cavitation occurs.

In compression, a similar set of equations can be used to describe the creep data:

$$\text{for} \quad |\sigma_a| > \beta \, \sigma_o \qquad |\dot{\epsilon}_s| = \lambda \, |\dot{\epsilon}_o| \, (|\sigma_a|/\beta \, \sigma_o)^N \tag{3a}$$

$$\text{for} \quad |\sigma_a| < \beta \, \sigma_o \qquad |\dot{\epsilon}_s| = \lambda \, |\dot{\epsilon}_o| \, (|\sigma_a|/\sigma_o)^n \tag{3b}$$

where β and λ are the ratios of compressive to tensile stress threshold and creep rates, respectively. It was found that the following parameter values fit the data quite well: $\dot{\epsilon}_o = 8\text{x}10^{-9}\ s^{-1}$, $\sigma_o = 100$ MPa, $\lambda = 0.1$, N = 10, n = 4 and $\beta = 2$.

To illustrate the major features of the asymmetric creep phenomena a model for the process is sketched in Figure 3. Fig. 3a shows a unit cell representative of the global creep behavior. The cell consists of two elements connected in parallel. One element contains two rigid grains with a tilted shear fault, symbolic of the interconnected SiC network during compression. The other element is a soft column, symbolic of the continuous silicon metal matrix, surrounding the rigid SiC particles. When the unit cell is stressed in tension, the load is carried mainly by the soft column as the other element is unable to carry any load due to the presence of cracks between contact sites of the silicon carbide grains. For $\sigma_a < \sigma_o$, deformation is a consequence of deformation of the silicon due to dislocation creep[5] (Fig. 3b). On the other hand, when $\sigma_a \geq \sigma_o$, the soft column is susceptible to cavitation damage between the silicon and the silicon carbide, Fig. 3c. Because the cavity volume contributes to the creep strain, this damage-enhanced creep results in an increase of stress sensitivity during creep. Rupture is eventually caused by the coalescence of these microvoids. This implies that the applied stress must be higher than the threshold, σ_o, for the rupture processes to occur. However, if the unit cell is stressed in compression, the crack does not have any effect on the load-carrying capacity of the composite and global compatibility requires the SiC element to take up most of the load because of its relative high rigidity. Overall deformation is then dictated by dislocation creep of SiC particles which also yields the same stress exponent as silicon, but at a much lower creep rate. At very high stresses, Fig. 3d, the friction barrier at the contact point along the shear crack is overcome and the sliding mechanism is activated leading to the enhancement of stress exponent.

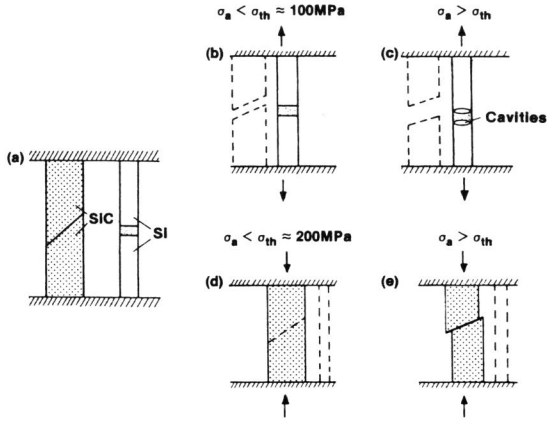

Figure 3. A simple mechanistic model for asymmetric creep: (a) representative unit of the composite; (b) tensile creep at stresses lower than a threshold, creep controlled by silicon, n = 4; (c) tensile creep above a threshold stress, cavitation leads to n = 10; (d) compressive creep at stresses less than a transitional stress, creep controlled by SiC, n = 4; (e) compressive creep above a transitional stress, creep controlled by sliding along a shear crack.

RUPTURE CRITERION

From extensive microstructural studies[5-6] of this material, damage evolution in KX01 is a consequence of cavitation at the interface between silicon and silicon carbide grains. The cavities are approximately the same size, d, as the SiC grains. With increasing cavity density, a critical strain is reached whereupon cavity coalescence takes place, forming large microcracks. Since microstructural analyses indicate that the microcracks are usually found only in those specimens tested to failure, the growth of these cracks to a critical size must occur rapidly. Thus, the critical strain at which cavity coalescence occurs is really an indication of a critical strain for failure.

Consistent with evidence provided in figure 1 (i.e. that lower creep rates result in longer lifetimes and higher creep strains at rupture), it is suggested that the critical crack size is proportional to the critical strain at rupture. Following this line of reasoning, an effective elastic fracture mechanics criterion may be applicable for lifetime predictions. In this model it is assumed that the critical strain, ϵ_{cr} is proportional to f(a) where f is some monotonically increasing function of crack length, a. To simplify the problem, f is assumed to be a linear function of crack

length[8], so that $\epsilon = \alpha a/d$, where α is a proportionality constant and the grain size d is employed for dimensional consistency. The constant α is of a statistical nature depending only on the heterogeneity of SiC grain distribution, the morphology of the two phase structure and other geometric factors. Hence, the best way to extract α is by experiment, as both ϵ_{cr} and a are measurable.

Figure 4 is an optical micrograph showing the enlarged rupture area of a tensile specimen crept at 125 MPa, 1300°C for 251 hrs. From observations of surface tinting, and cavity formation adjacent to the main crack, it is estimated that the crack length at rupture, a_{cr}, is about 1.02 mm. The final creep strain at rupture was ~0.61 percent, so α is estimated as $\sim 3 \times 10^{-5}$. Therefore, the proposed rupture criterion based on a critical strain to failure is given by the following equation:

$$\epsilon_{cr} = \frac{\alpha}{d} \, a_{cr} \tag{4}$$

This critical strain criterion will serve as a foundation on which the rupture time in both tensile and bending modes will be predicted in the following sections.

RUPTURE TIME UNDER TENSION

With the aid of Eqn (4), it is straightforward to derive the time to rupture, t_f, under uniaxial tensile creep. Assuming ϵ_f in equation (1) is equal to ϵ_{cr}, equation (1) and (4) can be combined to result in

$$a_{cr} = \dot{\epsilon}_s \, t_f \, d/\alpha \tag{5}$$

As an effective "elastic" fracture mechanics concept is assumed to apply, from which the following equation relating toughness, K_{IC}, σ_a and a_{cr} is obtained:

$$K_{IC} = \sigma_a \sqrt{8\pi a_{cr}} \tag{6}$$

where a factor of 8 is introduced as a result of interaction between a long edge crack and the finite width of the specimen as observed in Figure 4[2]. It should be noted that the estimated $a_{cr} \approx 1.00$ mm in Fig. 4 satisfies this equation for $K_{IC} = 20$ MPa$\sqrt{m}$ and $\sigma_a = 125$ MPa. This value of K_{IC} is consistent with values obtained on the material studied[10]. Substituting a_{cr} from Eqn (5) and σ_a from Eqn (2) into Eqn (6),

$$\dot{\epsilon}_s^{\,1+(2/N)} \, t_f = \frac{\alpha}{8\pi d} \, \dot{\epsilon}_o^{\,2/N} \left(\frac{K_{IC}}{\sigma_o} \right)^2 \tag{7}$$

This is a derived Monkman-Grant type equation relating $\dot{\epsilon}_s$ to t_f. It is shown that the exponent for $\dot{\epsilon}_s$ is no longer unity, so that the original Monkman-Grant formula applied successfully to metallic materials probably needs to be modified as indicated in Eqn (7) for ceramic materials.

To verify this theoretical prediction, a series of creep rupture tests under simple tension was carried out and the rupture data are reported in

[2]This was obtained from $K_I = Y \sigma_a \sqrt{a}$ [9] for an edge crack where $Y = 1.99 - 0.41\,x + 18.7\,x^2 - 38.45\,x^3 + 53.85\,x^4$ for $x = a/w \approx 0.5$, w being the width of the panel.

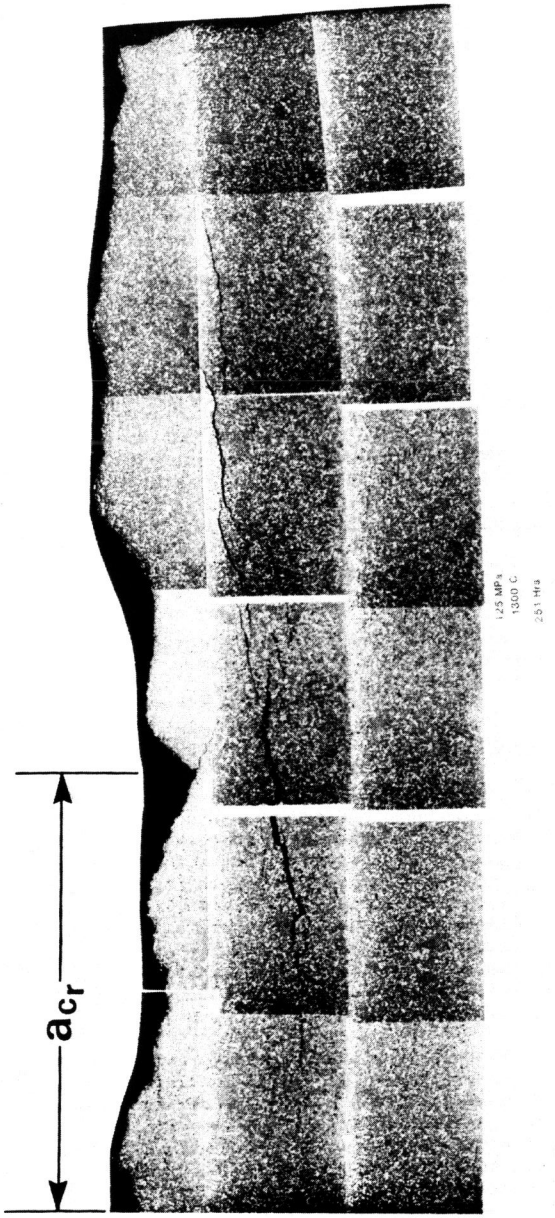

Figure 4. Optical micrograph of a tensile rupture zone of KX01 showing the relationship between critical crack size and final rupture strain. (Tensile axis vertical; $a_{cr} \approx 1.02$ mm, total width = 3 mm).

Figure 5. Using the following constants for Si/SiC at 1300°C, N = 10, d = 5 μm, $\alpha = 3\text{x}10^{-5}$, $\dot{\epsilon}_o = 8\text{x}10^{-9}\ s^{-1}$, σ_o = 100 MPa and K_{IC} = 20 MPa $\sqrt{m}$ [10], Eqn (7) becomes $\dot{\epsilon}_s^{1.2}\ t_f = 0.235\text{x}10^{-3}$. This equation is compared in figure 5 with the stress rupture data. Agreement between theory and experiment is good, not only in terms of the slope of the curve but also in absolute magnitude.

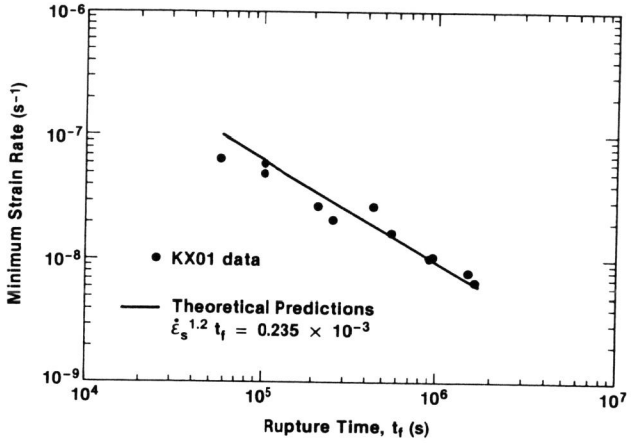

Figure 5. Correlation of analytical predictions and rupture data on the Monkman-Grant relationship in simple tension.

RUPTURE TIME UNDER BENDING

An understanding of the creep and creep rupture behavior of ceramic materials in bending is important because components or substructure such as beams, turbine blades, etc. are frequently subjected to bending. Furthermore, material evaluation and property characterization are generally conducted are flexure to avoid the complexity of specimen gripping and alignment of ceramics. In this section, rupture behavior in terms of lifetime predictions as a function of applied bending moment or displacement rate at the loading points ($\dot{\Delta}_p$) will be analyzed and compared to the rupture data collected. It will be shown that predictions of specimen lifetime in flexure can be based on an understanding of creep and creep rupture behavior in tension and compression.

The mechanics of flexural creep were investigated previously[4,11] for asymmetric creep materials obeying the constitutive laws of Eqns (2-3). The important results are summarized here; the reader is referred to ref. [4,11] for details. Using a methodology originally developed by Cohrt, et al.[12], which treats each fiber of the beam as a Maxwell element, time-dependent stress and strain distributions across the beam height are solved for a given bending moment (appropriate to the inner span of a four-point bend specimen). The results show that, under the conditions of constant moment and net zero forces, the local bending stresses

redistribute from the initial linear (elastic) distribution to a final non-linear (quasi-steady state creep) distribution within a time frame determined by a material constant, t_o, defined by[4,11]

$$t_o = \frac{\epsilon_{el}/\dot{\epsilon}_o}{\lambda Q^n} \tag{8}$$

where ϵ_{el} (= σ_a/E) is the initial outerfiber elastic strain and Q (= σ_a/σ_o) is the nondimensional applied stress normalized against σ_o. Moreover, as a consequence of stress redistribution, a prolonged transient period for bending creep results. This phenomenon is consistent with the bending creep curves collected in the laboratory[4]. On the other hand, the normal strain distribution along the beam height is always linear in agreement with Bernoulli's hypothesis, although the position of zero strain, H_ϵ, is not stationary. The prediction that the neutral strain axis migrates from the original geometric center towards the compression side as the creep test proceeds was confirmed experimentally[7,11].

With the availability of the time-dependent stress and strain solutions and a rupture criterion, it is possible to compute the rupture time. Based on the observed rupture behavior of a bend bar, it is suggested that somewhere in the inner span a major crack will emerge and "grow" from the tensile edge of the beam towards the center in accord with the strain criterion set out by Eqn (4). Because of strain linearization at all times, we can then compute t_f solely from the time-dependent solution of the strain at the tensile edge $\epsilon^*(t)$. It can be shown from a simple geometric sketch (figure 6) that the following relationship exists between the critical crack length at rupture, a_{cr}, and the outer fiber tensile strain, $\hat{\epsilon}^*_{cr}$ at rupture:

$$\hat{\epsilon}^*_{cr} = \frac{\alpha\ a_{cr}\ H\ (1-h_\epsilon)}{d\ [H(1-h_\epsilon) - a_{cr}]} \tag{9}$$

where H is the total beam height and h_ϵ is the location of zero strain as measured from the compressive edge normalized against H; a carat on top of ϵ means that the parameter is normalized against ϵ_{el}. The governing differential equation for the unknown $\epsilon^*(t)$ is

$$d\hat{\epsilon}^* = (6m - 2f)\ d\hat{t} \tag{10a}$$

subject to the initial condition

$$\hat{\epsilon}^*\ (\hat{t} = o) = 1 \tag{10b}$$

Here, m and f are functions of current stress state and the asymmetrical creep laws (cf. Eqns (11) of Ref. [11]); and $\hat{t} = t/t_o$ is the dimensionless time.

Having documented the necessary control equations, the time to rupture can be computed numerically from the following algorithm. For a given sustained load or bending moment, the critical crack length, a_{cr}, at which rupture takes place can be solved numerically by inverting the following nonlinear algebraic equation relating K_I to a and applied moment, M:[13]

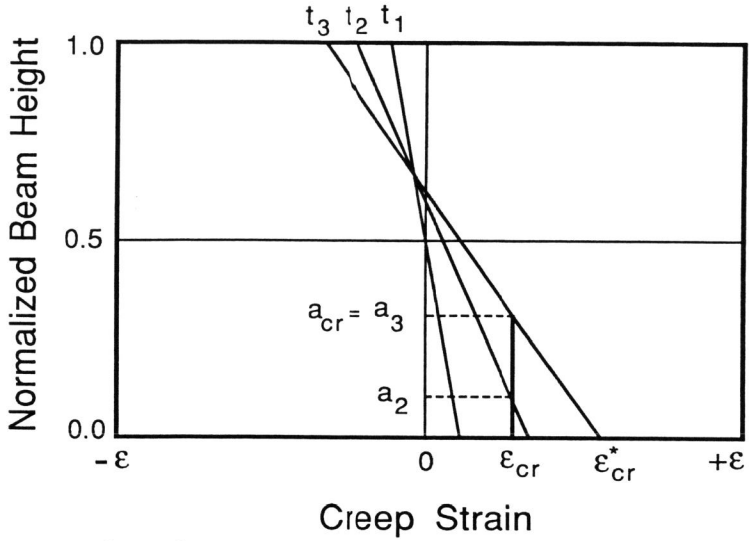

Figure 6. Schematic diagram showing the "growth" of the critical crack in a bend bar. At time t_1, there is no effective crack because the strain at the tensile edge, ϵ^*, is smaller than ϵ_{cr}; at time t_2, the length of the effective crack is a_2, while at time t_3, the crack size a_3 has reached a_{cr} and failure occurs.

$$K_I = \frac{6M/H}{BH^2} Y(a/H) \qquad (11)$$

where B is the beam width and $Y(x) = \sqrt{2}\tan\theta[0.923+0.199(1-\sin\theta)^4]/\cos\theta$; $\theta = \pi x/2$. When $K_I = K_{IC}$, a_{cr} can be determined. It should be noted that there are two solutions for this inversion problem, but only one, giving the higher a_{cr} for higher K_{IC}, is physically meaningful. With a_{cr} known together with the solution of $h_\epsilon(t)$, ϵ^* can be computed from Eqn (9). Finally, the initial-value problem of Eqn (10) is solved for ϵ^* and the time when ϵ^* reaches ϵ^*_{cr} is set for t_f; that terminates the computation.

A FORTRAN program was developed according to the numerical scheme described above. The input includes σ_a and other relevant material constants; the output is t_f. A single load input takes approximately 10 CPU seconds on the Cyber 855 supercomputer. A creep rupture type equation relating t_f to σ_a is plotted in Figure 7 for σ_a ranging from 200 to 400 MPa. The theoretical predictions of the solid line were computed at a load interval of 5 MPa beginning from σ_a = 200 MPa and ending at 400 MPa. The following material constants were also used as input: E = 350 GPa, K_{IC}, n, N, λ, σ_o and $\dot{\epsilon}_o$ same as before. It is observed that the solid line has a mild nonlinearity but for practical purposes, may be assumed linear in the double logarithmic space. The rupture data were

also presented in the same plot. Although the data show some scatter due to materials variation, the comparison indicates excellent agreement.

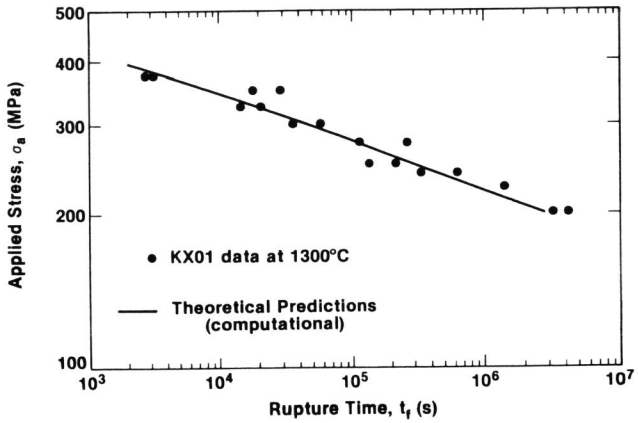

Figure 7. Correlation of numerical predictions and rupture data on the Larsen-Miller type relationship in bending.

CONCLUSION

We have presented analytical and numerical solutions of rupture behavior under tensile and bending creep conditions. Comparisons with creep rupture data under the appropriate conditions show that agreement is excellent. The theory was derived from a single rupture criterion based on a critical tensile strain. The results suggest that both tensile and bending rupture are dictated by the same rupture strain and that the creep and rupture processes are intimately coupled and thus inseparable. Finally, the present work demonstrates that the conventional wisdom of treating ceramic bend bars with symmetric creep equations may lead to erroneous results. More careful treatment in flexural creep is essential for characterization of long term behavior when ceramic composites are subject to bending.

ACKNOWLEDGEMENT

This work was supported by the U.S. Department of Energy, Advanced Heat Engines Program under Interagency Agreement DE-AI05-85OR21569.

REFERENCES

[1] Conway, J.B. and Flagella, P.N.: "Creep-Rupture Data for the Refractory Metals to High Temperatures", Gordon and Breach Sci. Publishers, New York, 1971.

[2] Jones, D.I.G.: "Stress Rupture of Ceramics: Time-Temperature Relationships", paper No. 87-GT-81, ASME Gas Turbine Conf. Anaheim, CA 1987.

[3] Wiederhorn, S.M., Roberts, D.E., Chuang, T.-J. and Chuck, L.: "Damage Enhanced Creep in a Siliconized Silicon Carbide: Phenomenology", J. Am Ceram. Soc., 71, pp 602-608, 1988.

[4] Chuang, T.-J. and Wiederhorn, S.M.: "Damage Enhanced Creep in a Siliconized Silicon Carbide: Mechanics of Deformation", J. Am. Ceram. Soc., 71, pp 595-601, 1988.

[5] Hockey, B.J. and Wiederhorn, S.M.: "Creep Deformation of Siliconized Silicon Carbide" to be published.

[6] Wiederhorn, S.M., Chuck, L., Fuller, E.R. and Tighe, N.J.: "Creep Rupture of Siliconized Silicon Carbide" in Tailoring Multiphase and Composite Ceramics, Eds. Tressler, R.E., Messing, G.L., Panrago and Newnham, R.E. pp 755-773, Plenum, New York, 1986.

[7] Chen, C.F.: "Creep Behavior of Sialon and Siliconized SiC Ceramics" Ph.D. Thesis, University of Michigan, Ann Arbor, MI 1987.

[8] Carroll, D.F.: "Creep Deformation of a Siliconized Silicon Carbide" Ph.D. Thesis, Penn State Univ., Univ. Park, PA, 1987.

[9] Broek, D.: "Elementary Engineering Fracture Mechanics" p. 76, 3rd Edition, Martinus Nijhoff, The Hague, Netherlands, 1983.

[10] Carroll, D.F., Chuang, T.-J. and Wiederhorn, S.M.: "A Comparison of Creep Rupture Behavior in Tension and Bending" Ceramic Eng. & Sci. Proc. in Press.

[11] Chuang, T.-J., Wiederhorn, S.M. and Chen, C.F.: "Transient Behavior of Structural Ceramics under Flexural Creep" pp 957-73 in Proc. Third Int. Conf. Creep and Fracture of Eng. Mater. & Structures, Eds. Wilshire, B., and Evans, R.W., The Inst. Metals, London, 1987.

[12] Cohrt, H., Grathwohl, G. and Thümmler: "Non-stationary Stress Distribution in a Ceramic Bending Beam during Constant Load Creep" Res. Mechanica, 10, pp. 55-71, 1984.

[13] Tada, H., Pans, P.C. and Irwin, G.R.: "The Stress Analysis of Cracks Handbook" pp 2-14, Del Research Corp. Hellertown, PA, 1973.

[14] Chuang, T.-J.: "Estimation of Power-law Creep Parameters from Bend Test Data" J. Mater. Sci. 21, pp 165-75, 1986.